

A Review of Three-Phase Connected Inverters for Photovoltaic Modules

Naramula.Roja

M.Tech(EPS),

Arjun College of Technology and Sciences.

S.Chandra Mouli, M.Tech

Assistant Professor,

Arjun College of Technology and Sciences.

ABSTRACT:

This paper displays a measured full H-bridge multilevel photovoltaic (PV) inverter for single-or three-stage lattice associated applications. The measured full multilevel topology enhances the effectiveness and adaptability of PV frameworks. To acknowledge better usage of PV modules and augment the sunlight based vitality extraction, a dispersed most extreme force point following control plan is connected to both single-and three-stage multilevel inverters, which permits free control of every dc-link voltage. For three-stage network associated applications, PV crisscrosses may present lopsided supplied power, prompting uneven lattice current. To fathom this issue, a control plan with regulation pay is additionally proposed. A trial three-stage seven-level full H-bridge inverter has been fabricated using nine H-bridge modules (three modules for each stage). Every H-bridge module is associated with a 185-W sunlight based board. Reenactment and trial results are displayed to check the achievability of the proposed approach.

Index Terms:

Cascaded multilevel inverter, distributed maximum power point (MPP) tracking (MPPT), modular, modulation compensation, photovoltaic (PV).

I. INTRODUCTION:

Because of the deficiency of fossil energizes and natural issues brought on by traditional force era, renewable vitality, especially sun oriented vitality, has turned out to be extremely prominent. Sun oriented electric-vitality request has become reliably by 20%–25% for every annum in the course of recent years [1], and the development is generally in framework associated applications.

With the remarkable business sector development in matrix associated photovoltaic (PV) frameworks, there are expanding interests in network associated PV configurations. Five inverter families can be defined, which are related to different configurations of the PV system: 1) central inverters; 2) string inverters; 3) multistring inverters; 4) ac-module inverters; and 5) cascaded inverters [2]–[7]. The configurations of PV systems are shown in Fig. 1.

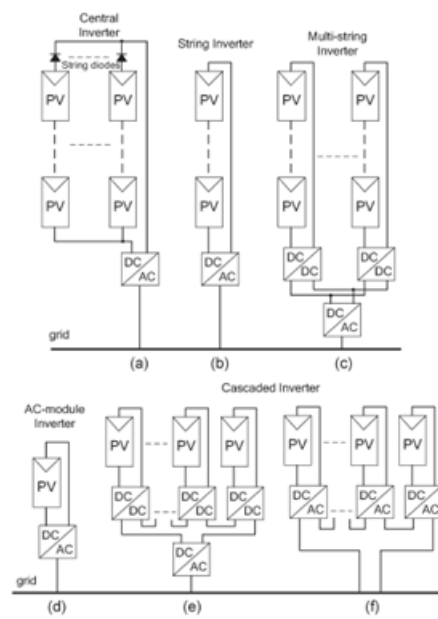


Fig. 1. Configurations of PV systems. (a) Central inverter. (b) String inverter. (c) Multistring inverter. (d) AC-module inverter. (e) Cascaded dc/dc converter. (f) Cascaded dc/ac inverter.

Full inverters comprise of a few converters associated in arrangement; in this way, the high power and/or high voltage from the mix of the different modules would support this topology in medium and substantial matrix associated PV frameworks [8]–[10].

There are two sorts of fell inverters. Fig. 1(e) demonstrates a fell dc/dc converter association of PV modules [11], [12]. Each PV module has its own particular dc/dc converter, and the modules with their related converters are still associated in arrangement to make a high dc voltage, which is given to an adjusted dc/air conditioning inverter. This methodology joins parts of string inverters and air conditioning module inverters and offers the upsides of individual module most extreme force point (MPP) following (MPPT), yet it is not so much immoderate but rather more productive than air conditioning module inverters. Be that as it may, there are two force transformation stages in this arrangement. Another fell inverter is appeared in Fig. 1(f), where each PV board is associated with its own particular dc/air conditioning inverter, and those inverters are then set in arrangement to achieve a high-voltage level [13]–[16]. This fell inverter would keep up the advantages of "one converter for each board, for example, better usage per PV module, ability of blending diverse sources, and excess of the framework.

Also, this dc/air conditioning fell inverter expels the requirement for the per-string dc transport and the focal dc/air conditioning inverter, which further enhances the general effectiveness. The particular fell H-span multilevel inverter, which requires a segregated dc hotspot for every H-extension, is one dc/air conditioning fell inverter topology. The different dc joins in the multilevel inverter make free voltage control conceivable. Thus, individual MPPT control in each PV module can be accomplished, and the vitality collected from PV boards can be amplified. In the interim, the measured quality and minimal effort of multilevel converters would position them as a prime contender for the up and coming era of effective, hearty, and solid framework associated sunlight based force gadgets. A particular fell H-span multilevel inverter topology for single-or three-stage lattice associated PV frameworks is introduced in this paper. The board confound issues are tended to demonstrate the need of individual MPPT control, and a control plan with conveyed MPPT control is then proposed.

The appropriated MPPT control plan can be connected to both single-and three-stage frameworks. Moreover, for the displayed three-stage network associated PV framework, if each PV module is worked at its own MPP, PV bangles may acquaint unequal force supplied with the three-stage multilevel inverter, prompting lopsided infused lattice current. To adjust the three-stage network current, balance pay is likewise added to the control framework. A three-phase modular cascaded multilevel inverter proto-type has been built. Each H-bridge is connected to a 185-W solar panel. The modular design will increase the flexibility of the system and reduce the cost as well. Simulation and experimental results are provided to demonstrate the developed control scheme.

II. SYSTEM DESCRIPTION:

Measured fell H-span multilevel inverters for single-and three-stage lattice associated PV frameworks are appeared in Fig. 2. Each stage comprises of n H-span converters associated in arrangement, and the dc connection of every H-scaffold can be bolstered by a PV board or a short string of PV boards. The fell multilevel inverter is associated with the matrix through L channels, which are utilized to lessen the exchanging music in the current. By various blends of the four switches in every H-span module, three yield voltage levels can be produced: $-v_{dc}$, 0, or $+v_{dc}$. A fell multilevel inverter with n inputsources will give $2n + 1$ levels to integrate the air conditioner yield waveform. This $(2n + 1)$ - level voltage waveform empowers the diminishment of sounds in the integrated current, lessening the span of the required yield channels. Multilevel inverters likewise have different focal points, for example, diminished voltage weights on the semiconductor switches and having higher effectiveness when contrasted with other converter topologies [17].

III. PANEL MISMATCHES:

PV confuse is a vital issue in the PV framework. Because of the unequal got irradiance, diverse temperatures, and maturing of the PV boards, the MPP of each PV module might be distinctive.

On the off chance that each PV module is not controlled freely, the effectiveness of the general PV framework will be diminished.

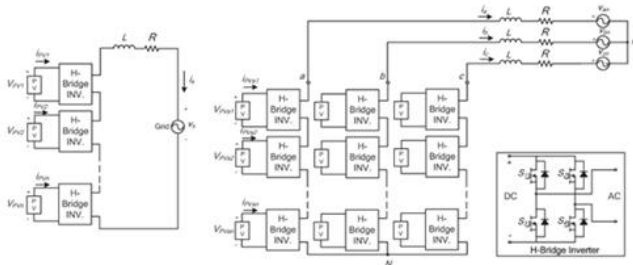


Fig. 2. Topology of the modular cascaded H-bridge multilevel inverter for grid-connected PV systems

Astronomy CHSM-5612M. Consider a working condition that every board has an alternate light from the sun; board 1 has irradiance $S = 1000 \text{ W/m}^2$, and board 2 has $S = 600 \text{ W/m}^2$. In the event that lone board 1 is followed and its MPPT controller decides the normal voltage of the two boards, the force extricated from board 1 would be 133 W, and the force from board 2 would be 70 W, as can be found in Fig. 3. Without individual MPPT control, the aggregate force reaped from the PV framework is 203 W. Nonetheless, Fig. 4 demonstrates the MPPs of the PV boards under the diverse irradiance. The greatest yield power qualities will be 185 and 108.5 W when the S qualities are 1000 and 600 W/m^2 , separately, which implies that the aggregate force collected from the PV framework would be 293.5 W if individual MPPT can be accomplished. This higher worth is around 1.45 times of the one preceding. In this way, individual MPPT control in each PV module is required to expand the productivity of the PV framework. In a three-stage framework associated PV framework, a PV befuddle may bring about more issues. Beside diminishing the general proficiency, this could even acquaint uneven force supplied with the three-stage lattice associated framework. In the event that there are PV mis-matches between stages, the info force of every stage would be distinctive. Since the lattice voltage is adjusted, this distinction in information force will bring about unbalanced current to the grid, which is not allowed by grid standards.

For example, to unbalance the current per phase more than 10% is not allowed for some utilities, where the percentage imbalance is calculated by taking the maximum deviation from the average current and dividing it by the average current [18].

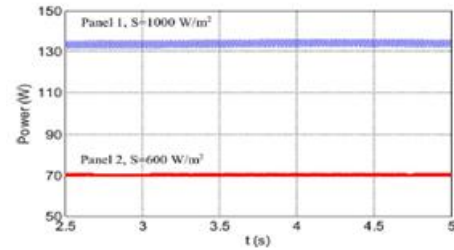


Fig. 3. Power extracted from two PV panels.

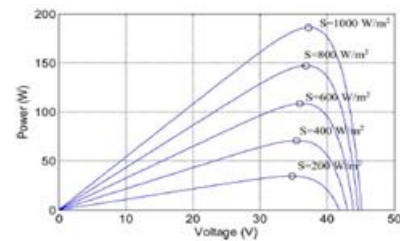


Fig. 4. P –V characteristic under the different irradiance.

To solve the PV mismatch issue, a control scheme with individual MPPT control and modulation compensation is pro-posed. The details of the control scheme will be discussed in the next section.

IV. CONTROL SCHEME

A. Distributed MPPT Control

Keeping in mind the end goal to dispose of the unfriendly impact of the crisscrosses and increment the proficiency of the PV framework, the PV modules need to work at various voltages to enhance the usage per PV module. The different dc joins in the fell H-span multilevel inverter make free voltage control conceivable. To genuinize individual MPPT control in each PV module, the control plan proposed in [19] is upgraded for this application. The disseminated MPPT control of the three-stage fell H-span inverter is appeared in Fig. 5. In every H-span module, a MPPT controller is added to produce the dc-join voltage reference.

Every dc-join voltage is contrasted with the comparing voltage reference, and the total of all mistakes is controlled through an aggregate voltage controller that decides the present reference I_{dref} . The responsive current reference I_{qref} can be set to zero, or if receptive force remuneration is required, I_{qref} can likewise be given by a receptive current adding machine [20], [21]. The synchronous reference outline stage bolted circle (PLL) has been utilized to discover the stage edge of the framework voltage [22]. As the great control plan in three-stage frameworks, the matrix streams in abc directions are changed over to dq organizes and managed through proportional–integral (PI) controllers to create the regulation file in the dq facilitates, which is then changed over back to three stages. The conveyed MPPT control plan for the single-stage framework is almost the same. The aggregate voltage controller gives the greatness of the dynamic current reference, and a PLL gives the recurrence and stage edge of the dynamic current reference. The present circle then gives the balance list.

To make each PV module work at its own MPP, take stage a for instance; the voltages v_{dca2} to v_{dca1} are con-trolled exclusively through $n-1$ circles. Every voltage controller gives the balance record extent of one H-span module in stage a. After increased by the balance index of stage a, $n-1$ tweak records can be acquired. Additionally, the regulation list for the primary H-extension can be gotten by subtraction. The control plans in phases b and c are practically the same. The main distinction is that all dc-join voltages are directed through PI controllers, and n regulation list extents are acquired for each phase A stage moved sinusoidal heartbeat width balance exchanging plan is then connected to control the exchanging gadgets of every H-span. It can be seen that there is one H-span module out of N modules whose balance list is acquired by subtraction. For single-stage frameworks, $N = n$, and for three-stage frameworks, $N = 3n$, where n is the quantity of H-scaffold modules per phase. The reason is that N voltage circles are important to oversee diverse voltage levels on N H-extensions, and

one is the aggregate voltage circle, which gives the present reference. In this way, just $N - 1$ modulation files can be dictated by the keep going $N - 1$ voltage circles, and one adjustment record must be acquired by subtraction. Numerous MPPT techniques have been produced and actualized [23], [24]. The incremental conductance technique has been utilized as a part of this paper. It loans itself well to computerized control, which can without much of a stretch monitor past estimations of voltage and current and settle on all choices.

B. Modulation Compensation:

As mentioned earlier, a PV mismatch may cause more problems to a three-phase modular cascaded H-bridge multi-level PV inverter. With the individual MPPT control in each H-bridge module, the input solar power of each phase would be different, which introduces unbalanced current to the grid. To solve the issue, a zero sequence voltage can be imposed upon the phase legs in order to affect the current flowing into each phase [25], [26]. If the updated inverter output phase voltage is proportional to the unbalanced power, the current will be balanced. Thus, the modulation compensation block, as shown in Fig. 6, is added to the control system of three-phase modular cascaded multilevel PV inverters. The key is how to update the modulation index of each phase without increasing the complexity of the control system. First, the unbalanced power is weighted by ratio r_j .

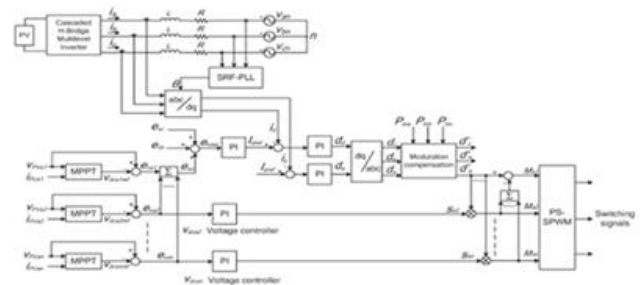


Fig. 5. Control scheme for three-phase modular cascaded H-bridge multilevel PV inverter.

$$r_j = \frac{P_{ina}}{P_{inj}} \quad (1)$$

where P_{inj} is the input power of phase j ($j = a, b, c$), and P_{inav} is the average input power. Then, the injected zero sequence modulation index can be generated as

$$d_0 = 2[\min(r_a \cdot d_a, r_b \cdot d_b, r_c \cdot d_c) + \max(r_a \cdot d_a, r_b \cdot d_b, r_c \cdot d_c)] - (2)$$

Where d_j is the modulation index of phase j ($j = a, b, c$) and is determined by the current loop controller. The modulation index of each phase is updated by

$$d'_j = d_j - d_0 \quad (3)$$

Only simple calculations are needed in the scheme, which will not increase the complexity of the control system. An example is presented to show the modulation compensation scheme more clearly. Assume that the input power of each phase is unequal

$$P_{ina} = 0.8P_{inb} = 1P_{inc} = 1. \quad (4)$$

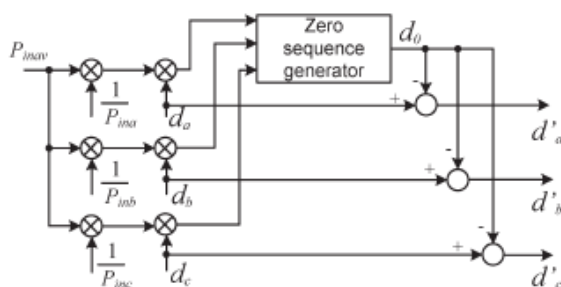


Fig. 6. Modulation compensation scheme.

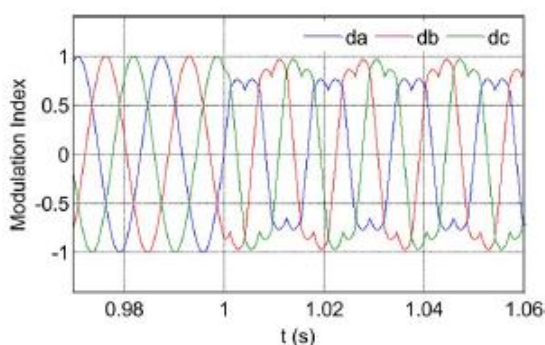


Fig. 7. Modulation indices before and after modulation compensation.

TABLE I: SYSTEM PARAMETERS

Parameters	Value
DC-link capacitor	3600 μ F
Connection inductor L	2.5 mH
Grid resistor R	0.1 ohm
Grid rated phase voltage	60 Vrms
Switching frequency	1.5 kHz

By injecting a zero sequence modulation index at $t = 1$ s, the balanced modulation index will be updated, as shown in Fig. 7. It can be seen that, with the compensation, the updated modulation index is unbalanced proportional to the power, which means that the output voltage (v_{jN}) of the three-phase inverter is unbalanced, but this produces the desired balanced grid current.

V. SIMULATION AND EXPERIMENTAL RESULTS:

Simulation Reproduction and test tests are completed to accept the proposed thoughts. A measured full multilevel inverter model has been inherent the research facility. The MOSFET IRFSL4127 is chosen as inverter switches working at 1.5 kHz. The control signs to the H-span inverters are sent by a dSPACE ds1103 controller. A three-stage seven-level full H-span inverter is recreated and tried. Every H-span has its own 185-W PV board (Astronergy CHSM-5612M) associated as a free source. The inverter is associated with the framework through a transformer, and the stage voltage of the auxiliary side is 60 Vrms. The framework parameters are appeared in Table I.

A. Simulation Results:

To confirm the proposed control conspire, the three-stage matrix associated PV inverter is reenacted in two unique conditions. To start with, all PV boards are worked under the same irradiance $S = 1000\text{W/m}^2$ and temperature $T = 25^\circ\text{C}$. At $t = 0.8\text{s}$, the sunlight based irradiance on the first and second boards of stage an abatements to 600W/m^2 , and that for alternate boards finishes what has been started. The dc-join voltages of stage are appeared in Fig. 8. Toward the starting, all PV boards are worked at a MPP voltage of 36.4 V.

As the irradiance changes, the first and second dc-join voltages abatement and track the new MPP voltage of 36 V, while the third board is still worked at 36.4 V. The PV current waveforms of stage an are appeared in Fig. 9. After $t = 0.8$ s, the streams of the first and second PV boards are much littler because of the low irradiance, and the lower swell of the dc-join voltage can be found in Fig.8(a).

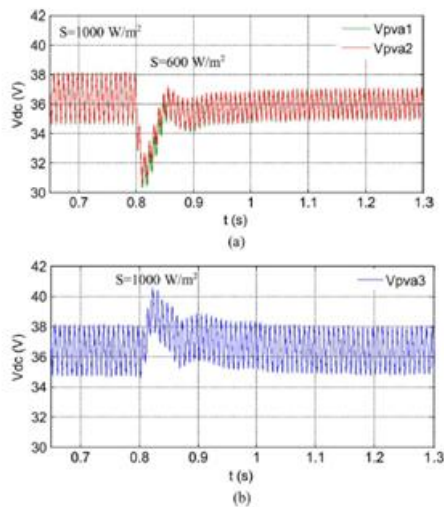


Fig. 8. DC-link voltages of phase a with distributed MPPT ($T = 25^\circ\text{C}$).DC-link voltage of modules 1 and 2. (b) DC-link voltage of module 3

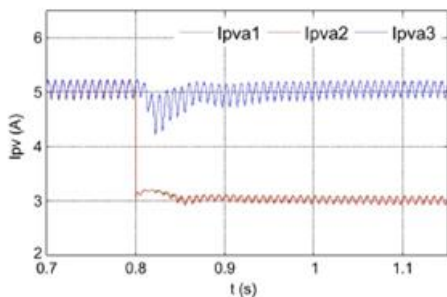


Fig. 9. PV currents of phase a with distributed MPPT ($T = 25^\circ\text{C}$).

The dc-link voltages of phase b are shown in Fig. 10. All phase-b panels track the MPP voltage of 36.4 V, which shows that they are not influenced by other stages. With the conveyed MPPT control, the dc-join voltage of every H-scaffold can be controlled freely. As it were, the associated PV board of every H-extension can be worked at its own MPP voltage and

won't be impacted by the boards associated with other H-spans. Hence, more sunlight based vitality can be extricated, and the productivity of the general PV framework will be increased. Fig. 11 demonstrates the force extricated from every stage. Toward the starting, all boards are worked under irradiance

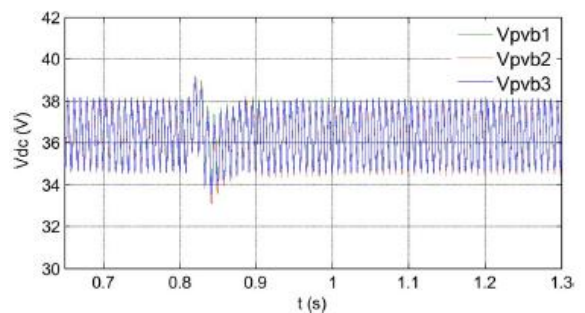


Fig. 10. DC-link voltages of phase b with distributed MPPT ($T = 25^\circ\text{C}$).

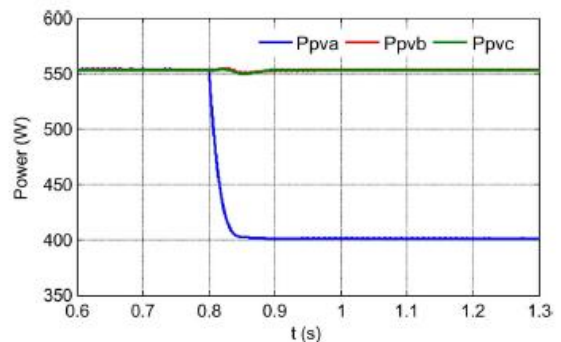


Fig. 11. Power extracted from PV panels with distributed MPPT.

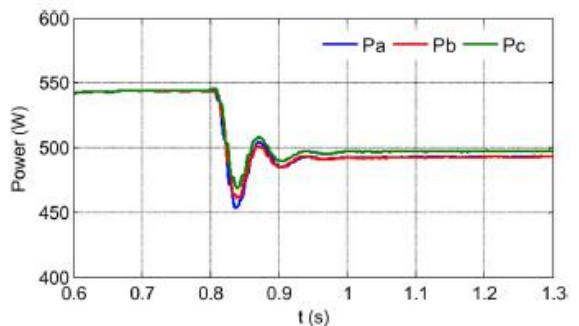


Fig. 12. Power injected to the grid with modulation compensation.

$S = 1000\text{W/m}^2$, and every phase is generating a maximum power of 555 W. After $t = 0.8$ s, the force gathered from stage an abatements to 400 W, and those from the other two stages keep with it. Clearly, the force supplied to the three-stage matrix associated inverter is lopsided. Nonetheless, by applying the adjustment pay plot, the force infused to the matrix is still adjusted, as appeared in Fig. 12. What's more, by contrasting the aggregate force separated from the PV boards with the aggregate force infused to the matrix, it can be seen that there is no additional force misfortune brought on by the adjustment remuneration scheme. Fig. 13 demonstrates the yield voltages (v_{jN}) of the three-stage inverter. Due to the infused zero arrangement segment, they are lopsided after $t = 0.8$ s, which adjust the lattice current appeared in Fig. 14.

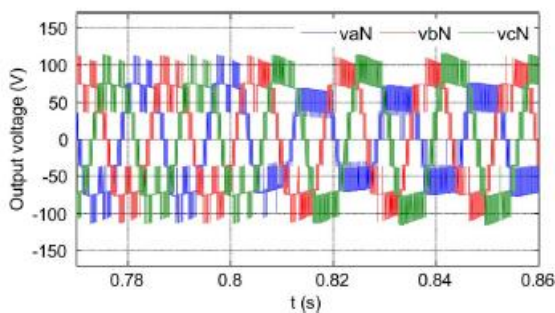


Fig. 13. Three-phase inverter output voltage waveforms with modulation compensation.

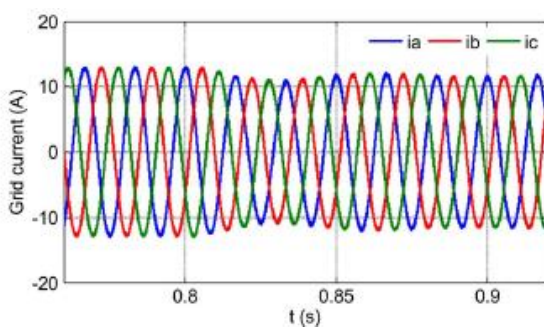


Fig. 14. Three-phase grid current waveforms with modulation compensation.

B. Experimental Verification:

A three-phase seven-level cascaded H-bridge inverter has been built by nine H-bridge modules (three modules per phase) in the laboratory.

Fig. 15 shows the experimental solar panels and the three-phase modular cascaded multilevel inverter. As mentioned previously, the dc link of each H-bridge module is fed by one PV panel Astronergy CHSM-5612M. To accept the proposed control conspire, the three-stage framework associated PV inverter has been tried under various conditions. In the tests, cards with various sizes are set on top of PV boards to give halfway shading, which viably changes the sun oriented irradiance. Test 1: A little blue card ($9\text{ cm} \times 7\text{ cm}$) is put on the third panel of stage an, and one cell of the board is incompletely secured, as appeared in Fig. 16. The trial results are exhibited in Figs. 17–21. Fig. 17 demonstrates three dc-join voltages of stage a. The yield voltage of each PV board is controlled exclusively to track its own particular MPP voltage. Since the third board is halfway secured, its MPP voltage is a little lower. The PV current waveforms of stage an are appeared in Fig. 18.

The PV current of the third board is littler because of the card covering. In any case, the first and second boards are worked at their own MPPs, and their PV streams are not affected. With the individual MPPT control, the productivity misfortune brought on by PV bungsles can be forestalled. As appeared in Fig. 17, there is a second-arrange symphonious in the yield voltage of the PV boards. In this way, the second-arrange symphonious is additionally found in the yield current of the PV boards. Moreover, to have a high use proportion of 99% of PV modules, the voltage swell ought to be under 6% of the MPP voltage [27]. In this test, the voltage swell is around 1.8 V, which is under 6% of the MPP voltage. Fig. 19 demonstrates the sun oriented force extricated from every stage, which is uneven. To adjust the infused matrix current, the balance remuneration plan proposed here is connected. As exhibited in Fig. 20, a zero grouping voltage is forced upon the stage legs. The inverter yield voltage (v_{jN}) is uneven corresponding to the supplied force of every stage, which adjusts the network current. Fig. 21 demonstrates the three-stage framework current waveforms.

Regardless of the fact that PV jumble happens and the supplied PV energy to the three-stage framework is unequal, the three-stage network current is still adjusted. The aggregate consonant contortion (THD) of the framework current appeared in Fig. 21 is 3.3%, as appeared in Fig. 22, which is under 5% and meets power quality benchmarks, as IEEE 1547 in the U.S. what's more, IEC 61727 in Europe.

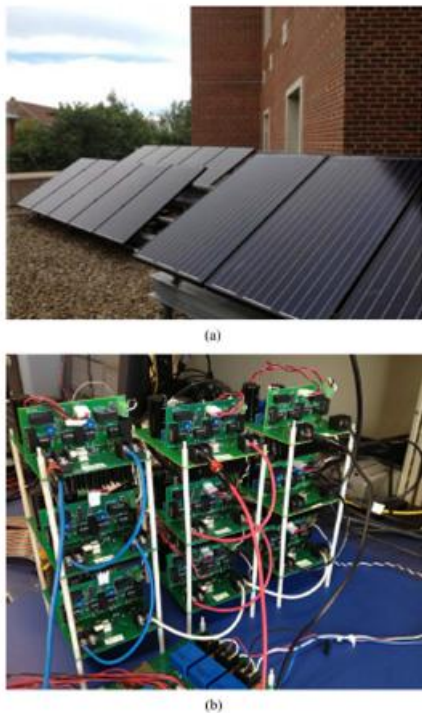


Fig. 15.Experimental prototype. (a) Solar panels Astronergy CHSM-5612M.(b) Modular three-phase seven-level cascaded H-bridge inverter.

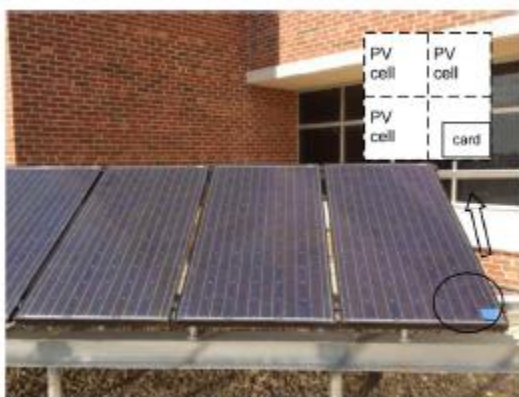


Fig. 16. PV panels of phase a: One cell of the third panel is partly covered.

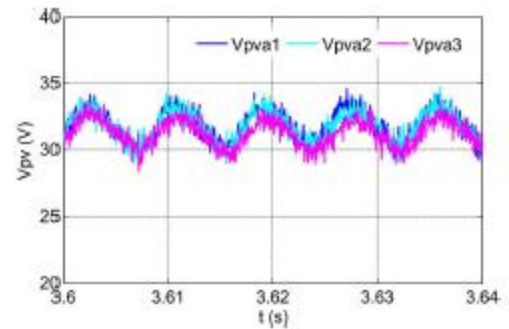


Fig. 17.Experimental dc-link voltages of phase a.

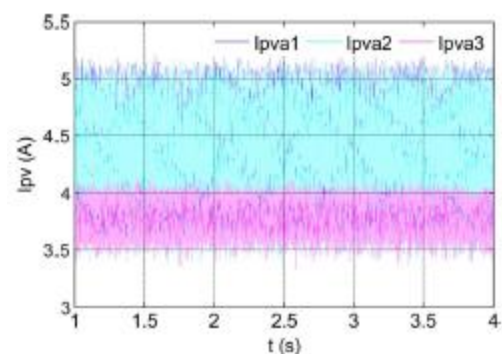


Fig. 18.Experimental PV currents of phase a (test 1).

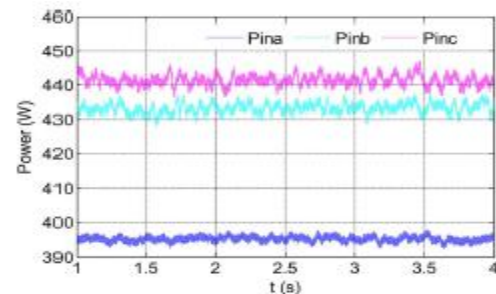


Fig. 19. Experimental power extracted from PV panels with distributed MPPT (test 1).

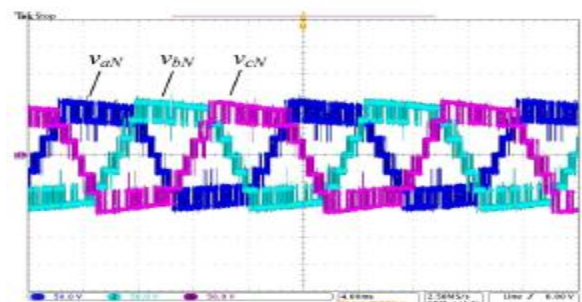


Fig.20. Experimental inverter output voltages with modulation compensation (test 1)

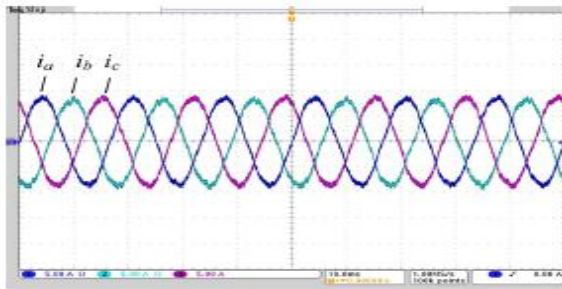


Fig. 21. Experimental grid currents with unbalanced PV power (test 1).

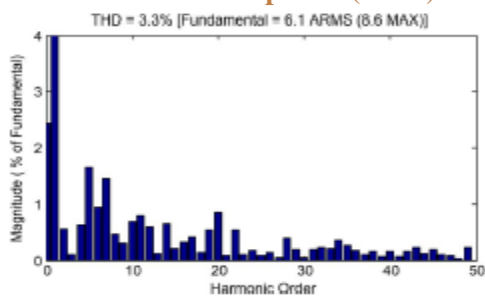


Fig. 22. THD of the grid current shown in Fig. 21 (test 1).



Fig. 23. PV panels of phase a: One cell of the third panel is covered.

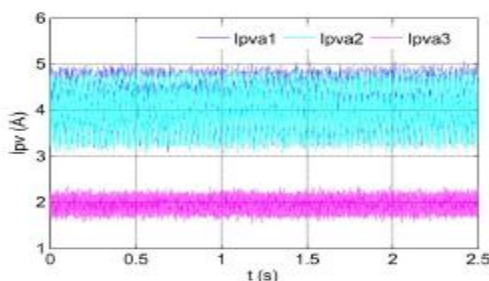


Fig. 24. Experimental PV currents of phase a (test 2).

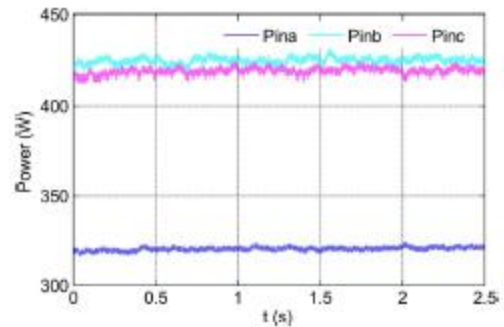


Fig. 25. Experimental power extracted from PV panels with distributed MPPT (test 2).

Test 2: A large blue card (13.5 cm × 9 cm) is placed on the third panel of phase a, and one cell of the panel is almost fully covered, as shown in Fig. 23. Fig. 24 shows the PV current waveforms of phase a. Since one cell of the third panel is almost fully covered, the current of the panel drops to 2 A, while the currents of the other two panels in the same phase are still 4 A. The harvested solar power of each phase is shown in Fig. 25. Compared to test 1, the power supplied to the three-phase system is more unbalanced. However, the three-phase grid current can still be balanced by applying the modulation compensation, as presented in Fig. 26. The THD of the grid current is 4.2%, and the rms value is 5.5 A. Fig. 27 shows the inverter output voltage waveforms. As discussed earlier, the inverter output voltage (v_{jN}) is unbalanced proportional to the supplied solar power of each phase to help balance the grid current. Thus, the output voltages v_{bN} (76.0 Vrms) and v_{cN} (75.2 Vrms) are higher than v_{aN} (57.9 Vrms).

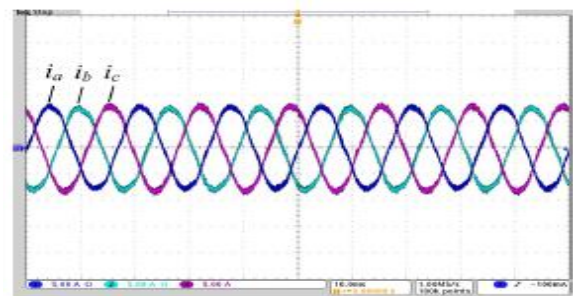


Fig. 26. Experimental grid currents with unbalanced PV power (test 2).

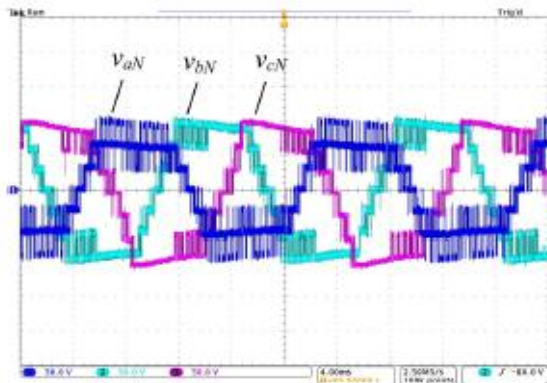


Fig. 27. Experimental inverter output voltages with modulation compensation (test 2).

VI. CONCLUSION:

In this paper, a measured full H-span multilevel inverter for matrix associated PV applications has been displayed. The multilevel inverter topology will enhance the use of associated PV modules if the voltages of the different dc connections are controlled autonomously. In this way, a conveyed MPPT control plan for both single-and three-stage PV frameworks has been connected to build the general proficiency of PV frameworks. For the three-stage lattice associated PV framework, PV befores may present uneven supplied power, bringing about un-adjusted infused matrix current. A regulation pay plan, which won't build the multifaceted nature of the control framework or cause additional force misfortune, is added to adjust the matrix current. A secluded three-stage seven-level full H-span inverter has been inherent the research facility and tried with PV boards under various incomplete shading conditions. With the proposed control conspire, each PV module can be worked at its own particular MPP to amplify the sun oriented vitality extraction, and the three-stage matrix current is adjusted even with the unequal supplied sun powered force.

ACKNOWLEDGMENT:

This work made utilization of the Engineering Research Center Shared Facilities bolstered by the Engineering Research Center Program of the National Science Foundation (NSF) and Department of Energy

under NSF Award EEC-1041877 and the Center for Ultra-Wide-Area Resilient Electric Energy Transmission Networks (CURENT) Industry Partnership Program.

REFERENCES:

- [1] J. M. Carrasco et al., "Power-electronic systems for the grid integration of renewable energy sources: A survey," *IEEE Trans. Ind. Electron.*, vol. 53, no. 4, pp. 1002–1016, Jun. 2006.
- [2] S. B. Kajar, J. K. Pedersen, and F. Blaabjerg, "A review of single-phase grid connected inverters for photovoltaic modules," *IEEE Trans. Ind. Appl.*, vol. 41, no. 5, pp. 1292–1306, Sep./Oct. 2005.
- [3] M. Meinhardt and G. Cramer, "Past, present and future of grid connected photovoltaic- and hybrid power-systems," in *Proc. IEEE PES SummerMeet.*, 2000, vol. 2, pp. 1283–1288.
- [4] M. Calais, J. Myrzik, T. Spooner, and V. G. Agelidis, "Inverter for single-phase grid connected photovoltaic systems—An overview," in *Proc. IEEE PES*, 2002, vol. 2, pp. 1995–2000.
- [5] J. M. A. Myrzik and M. Calais, "String and module integrated inverters for single-phase grid connected photovoltaic systems—A review," in *Proc. IEEE Bologna Power Tech Conf.*, 2003, vol. 2, pp. 1–8.
- [6] F. Schimpf and L. Norum, "Grid connected converters for photovoltaic, state of the art, ideas for improvement of transformer less inverters," in *Proc. NORPIE*, Espoo, Finland, Jun. 2008, pp. 1–6.
- [7] B. Liu, S. Duan, and T. Cai, "Photovoltaic DC-building-module-based BIPV system—Concept and design considerations," *IEEE Trans. Power Electron.*, vol. 26, no. 5, pp. 1418–1429, May 2011.

- [8] L. M. Tolbert and F. Z. Peng, "Multilevel converters as a utility interface for renewable energy systems," in Proc. IEEE Power Eng. Soc. SummerMeet., Seattle, WA, USA, Jul. 2000, pp. 1271–1274.
- [9] H. Ertl, J. Kolar, and F. Zach, "A novel multicell DC–AC converter for applications in renewable energy systems," IEEE Trans. Ind. Electron., vol. 49, no. 5, pp. 1048–1057, Oct. 2002.
- [10] S. Daher, J. Schmid, and F. L. M. Antunes, "Multilevel inverter topologies for stand-alone PV systems," IEEE Trans. Ind. Electron., vol. 55, no. 7, pp. 2703–2712, Jul. 2008.
- [11] G. R. Walker and P. C. Sernia, "Cascaded DC–DC converter connection of photovoltaic modules," IEEE Trans. Power Electron., vol. 19, no. 4, pp. 1130–1139, Jul. 2004.
- [12] E. Roman, R. Alonso, P. Ibanez, S. Elorduizapatarietxe, and D. Goitia, "Intelligent PV module for grid-connected PV systems," IEEE Trans. Ind. Electron., vol. 53, no. 4, pp. 1066–1073, Jun. 2006.
- [13] F. Filho, Y. Cao, and L. M. Tolbert, "11-level cascaded H-bridge grid-tied inverter interface with solar panels," in Proc. IEEE APEC Expo., Feb. 2010, pp. 968–972.
- [14] C. D. Townsend, T. J. Summers, and R. E. Betz, "Control and modulation scheme for a cascaded H-bridge multi-level converter in large scale photovoltaic systems," in Proc. IEEE ECCE, Sep. 2012, pp. 3707–3714.
- [15] B. Xiao, L. Hang, and L. M. Tolbert, "Control of three-phase cascaded voltage source inverter for grid-connected photovoltaic systems," in Proc. IEEE APEC Expo., Mar. 2013, pp. 291–296.
- [16] Y. Zhou, L. Liu, and H. Li, "A high-performance photovoltaic module-integrated converter (MIC) based on cascaded quasi-Z-source inverters (qZSI) using eGaN FETs," IEEE Trans. Power Electron., vol. 28, no. 6, pp. 2727–2738, Jun. 2013.
- [17] J. Rodriguez, J. S. Lai, and F. Z. Peng, "Multilevel inverters: A survey of topologies, controls, and applications," IEEE Trans. Ind. Electron., vol. 49, no. 4, pp. 724–738, Aug. 2002.
- [18] Standard for Electric Installation and Use. [Online]. Available: [https:// www.xcelenergy.com/](https://www.xcelenergy.com/)
- [19] A. Dell'Aquila, M. Liserre, V. Monopoli, and P. Rotondo, "Overview of PI-based solutions for the control of DC buses of a single-phase H-bridge multilevel active rectifier," IEEE Trans. Ind. Appl., vol. 44, no. 3, pp. 857– 866, May/Jun. 2008.
- [20] B. Xiao, K. Shen, J. Mei, F. Filho, and L. M. Tolbert, "Control of cascaded H-bridge multilevel inverter with individual MPPT for grid-connected photovoltaic generators," in Proc. IEEE ECCE, Sep. 2012, pp. 3715– 3721.
- [21] Y. Xu, L. M. Tolbert, J. N. Chiasson, F. Z. Peng, and J. B. Campbell, "Generalized instantaneous no active power theory for STATCOM," IETElect. Power Appl., vol. 1, no. 6, pp. 853–861, Nov. 2007.
- [22] V. Kaura and V. Blasko, "Operation of a phase locked loop system under distorted utility conditions," IEEE Trans. Ind. Appl., vol. 33, no. 1, pp. 58– 63, Jan./Feb. 1997.
- [23] T. Esum and P. L. Chapman, "Comparison of photovoltaic array maximum power point tracking techniques," IEEE Trans. Energy Convers., vol. 22, no. 2, pp. 439–449, Jun. 2007.



- [24] D. P. Hohm and M. E. Ropp, "Comparative study of maximum power point tracking algorithms," *Program. Photovoltaic., Res. Appl.*, vol. 11, no. 1, pp. 47–62, Jan. 2003.
- [25] S. Rivera et al., "Cascaded H-bridge multilevel converter multistring topology for large scale photovoltaic systems," in *Proc. IEEE ISIE*, Jun. 2011, pp. 1837–1844.
- [26] T. J. Summers, R. E. Betz, and G. Mirzaeva, "Phase leg voltage balancing of a cascaded H-bridge converter based STATCOM using zero sequence injection," in *Proc. Eur. Conf. Power Electron. Appl.*, Sep. 2009, pp. 1–10.
- [27] S. B. Kjaer, "Design and control of an inverter for photovoltaic applications," Ph.D. dissertation, Inst. Energy Technol., Aalborg University, Aalborg East, Denmark, 2004/2005.